Title

Critical Review of Thermal Conductivity Models for Unsaturated Soils

Journal

Geotechnical and Geological Engineering, 33(2)

ISSN

0960-3182

Authors

Dong, Y

McCartney, JS

Lu, N

Publication Date

2015-04-01

DOI

10.1007/s10706-015-9843-2

Peer reviewed

Critical Review of Thermal Conductivity Models for Unsaturated Soils

Yi Dong [1], John S. McCartney, P.E., M.ACSE [2], Ning Lu, F.ASCE [3]

January 9, 2014

[1]Post-doctoral fellow, Department of Civil & Environmental Engineering, Colorado School of Mines, 1012 14th St., Golden, CO 80401. Email: ydong@mines.edu
[2]Associate Professor, Department of Civil, Environmental, and Architectural Engineering, University of Colorado at Boulder, UCB 428, Boulder, CO 80309. Email: john.mccartney@colorado.edu

[3]Professor and corresponding author, Department of Civil & Environmental Engineering, Colorado School of Mines, 1012 14th St., Golden, CO 80401. Email: ninglu@mines.edu

Abstract Although it is well established that heat conduction in unsaturated soil depends on liquid saturation, there are several models available to consider the changes in thermal conductivity during drying and wetting. The key factors affecting thermal conductivity of unsaturated soil are evaluated through a critical examination of these different models and their development. Depending on the principles and assumptions employed, these models are categorized into three groups: mixing models involving series/parallel elements; empirical models where thermal conductivity values at dry and saturated states are used; and mathematical models based on phase volume fractions. Experimental data for different soils are used to assess the quality of prediction for these models. It is found that all the existing models do not realistically account for pore structure or interface properties, and thus are not capable of predicting thermal conductivity as a function of liquid saturation. A conceptual model based on soil-water retention mechanisms, is proposed to overcome the pitfalls of the existing models and can be used to establish quantitative thermal conductivity models for variably saturated soils in the future.

Keywords: Thermal conductivity, heat transfer, unsaturated soil, soil-water retention.

Introduction

Heat transfer in soil and rock presents a field of fertile research in which the thermal properties of soils are used in a large number of geotechnical, geophysical and geo-environmental applications, including geothermal energy resources (White, 1973), radioactive waste disposal (Li et al., 2012), ground-source heat pump systems (Preene and Powrie, 2009), energy piles (Brandl, 2006), geological CO_2 sequestration (Ebigbo, 2005) and recovery of natural methane gas hydrates (Cortes et al., 2009).

Soil is a multi-phase material consisting of solid particles, gas and/or liquid. Thermal properties of soils are not only determined by the intrinsic physical properties of each phase, but also affected by environmental variation of each phase. The thermal conductivity k of different soil phases varies over two orders of magnitude (e.g. thermal conductivity of mineral particles $k_{mineral} > 3$ W/m·K, thermal conductivity of water $k_{water} = 0.56$ W/m·K (at 0 ^{o}C), and thermal conductivity of air $k_{air} = 0.026$ W/m·K) (Mitchell and Soga, 2005; Yun and Santamarina, 2008). However, the thermal conductivity of dry soil k_{dry_soil} is almost one order of magnitude lower than that of the pure mineral solids, in most cases $k_{dry\_soil} < 0.5$ W/m·K, depending on mineral composition and packing density (Farouki, 1981). This implies that the air obstructs heat conduction and heat conduction primarily occurs through the particle contacts in dry soil. At the other end, the thermal conductivity of water-saturated soil is between that of the pure mineral and that of water, implying that replacement of air with water provides a significant improvement in the heat conduction through the soil mixture. The ordered sequence of typical thermal conductivity values are

$k_{air} < k_{dry\_soil} < k_{water} < k_{saturated\_soil} < k_{mineral}$. These observations, and many experimental studies (Brandon and Mitchell, 1989; Farouki, 1981; Smits et al., 2010), confirm that the varying water saturation in the soil mixture system plays an important role in determining the bulk thermal properties.

The purposes of this paper are: (1) to identify the controlling physical mechanisms for the thermal behavior of the soil at various unsaturated conditions, and (2) to assess the existing models for their predictability of thermal conductivity under varying saturation conditions.

Heat Transfer Mechanisms and Governing Factors

There are three heat transfer mechanisms in a material medium: conduction through solids and liquids, convection in fluids, and radiation (which does not require a material medium). The most effective means of transferring heat in dry particulate materials is through the solid contacts, while conduction through the gas phase and radiation have less relevant effects (Carslaw and Jaeger, 1959; Murashov and White, 2000). Heat transfer by convection plays an important role if the particle size D_{50} is larger than ~ 6 mm permitting fluid flow through the porous network (Yun, 2005). In this paper, the scope of our assessment of thermal conductivity models considers only heat transfer by conduction. It is assumed that soils are under room temperature and under a small temperature gradient. Thus, the liquid phase change or water vapor enhancement induced by high temperature and the heat flux of fluid convection due to high temperature gradient are ignored. Under these assumptions, the apparent or effective thermal

conductivity of soil is often used to describe the heat transfer capability of multi-phase materials.

The heat flux q [W/m^2] at steady state is proportional to the thermal gradient by the coefficient of thermal conductivity k [W/mK], according to the constitutive equation of Fourier's law in one dimension:

$$q = k \cdot \frac{dT}{dx} \tag{1}$$

The rate of heat transfer in transient conditions is equal to the heat stored within the medium and the rate of internal heat generation, given by the continuity equation:

$$\frac{dq}{dx} = q_{\text{generated}} - q_{\text{stored}} \tag{2}$$

where the heat stored in the material is: $q_{\text{stored}} = \rho \cdot c \cdot (\partial T / \partial t)$, ρ [kg/m^3] is the material mass density, and c [J/kgK] is the heat capacity. If there is no heat generation within the material, the $q_{\text{generated}}$ term vanishes. Combining the above two equations leads to Fick's second law:

$$\frac{\partial^2 T}{\partial x^2} = -D \frac{\partial T}{\partial t} \tag{3}$$

where $D = k/(\rho \cdot c)$ [m^2/s] is the thermal diffusivity which reflects how fast heat will be transferred through a material. The negative sign indicates that heat transfer occurs in the direction opposite to the temperature gradient. Common values of thermal conductivity,

diffusivity, and specific heat of different soils and their phase components are summarized in Table 1.

The thermal properties of soils under isothermal conditions are governed by several particle-level and macro-scale factors: mineralogy, particle size, particle shape, packing geometry, stress level, water content, porosity, gradation, and cementation.

Mineralogy. Solid minerals are the most conducive constituents in the air-water-solid soil system; thus they define the upper limit of the thermal conductivity. Soil comprised of different mineral substances has different thermal conductivity (e.g., quartz > mica) (Gangadhara Rao and Singh, 1999; Tarnawski et al., 2002). Soil with higher quartz content has larger thermal conductivity values (Tarnawski et al., 2009).

Particle size and gradation. Heat flux between particles is proportional to the radius of the particles. Larger particles and fewer contacts in a given volume result in higher thermal conductivity (Aduda, 1996; Gangadhara Rao and Singh, 1999). Well-graded soil exhibits higher heat transfer as small particles fill the interstitial pore space and increases the inter-particle coordination (Esch, 2004).

Packing geometry. Higher inter-particle coordination increases the thermal conductivity for a given particle size (Lambert and Fletcher, 1997b; Tarnawski et al., 2002). The contact conductance is more important than the radiational conductance (Lambert and Fletcher, 1997a). The thermal conduction at contacts results in percolation-type conduction process (Sahimi and Tsotsis, 1997).

Stress level. Higher stress results in higher contact radii leading to an increase in thermal conductivity therefore thermal conductivity. Granular chains under higher stress also gives rise to more developed heat transfer paths (Vargas and McCarthy, 2001).

Water content. Fluid volume fraction is a dominant factor to the thermal conductivity in partially saturated soils. At residual water content region, adding small amount of water dramatically improves the thermal conduction. The increase of thermal conductivity with increase of water content in unsaturated soils suggests the important role of the pore fluid conduction (Singh and Devid, 2000).

Porosity. The lower the void ratio, the higher the thermal conductivity (Brandon and Mitchell, 1989; Yun and Santamarina, 2008).

Cementation. Cement and colloidal precipitation at particle contacts increases the contact area and thus increase the thermal conductivity (Tarnawski et al., 2002).

Through the analysis of these factors affecting the effective thermal conductivity of soils found in the literature, they can be generalized into few essential elements: thermal conductivity of each constituent (i.e., minerals, liquid, and air), water content, soil type (e.g., particle size/shape), and particle contacts (e.g., coordination numbers), which can be affected in a number of macro-level manifestation such as porosity, stress level, and gradation. The key governing factors are summarized in Table 2.

Thermal Conductivity Models

The accurate prediction of the thermal conductivity of composite materials comprises a significant portion of the literature about heat transfer in porous media, and a large number of effective thermal conductivity models have been proposed. New models for thermal conductivity of soils are emerging, suggesting that, to-date, a unified model or prediction procedure has not been found with universal applicability. In this section, several existing models have been reviewed and categorized into the following three groups based upon their principles:

Mixing models. This type of model conceptualizes the multi-phase soil system as a certain combination of series and parallel solid, air and/or water blocks in the cubic cell or representative elementary volume (REV); and the effective thermal conductivity of the bulk medium is calculated by mixing those blocks.

Empirical models. This group of models builds the relationship between relative thermal conductivity and degree of saturation or water content, by normalizing the effective thermal conductivity or Kersten number over the difference between saturated state thermal conductivity k_{sat} and dry state thermal conductivity k_{dry}.

Mathematic models. These models were adopted from predictive models of other physical properties, such as dielectric permittivity, magnetic permeability, electrical conductivity, and hydraulic conductivity; which are calculated by certain mathematical algorithm given the thermal conductivity of each component and their volume fractions.

Mixing Models

The most common models are based on classical mixing laws (arithmetic and harmonic) of series model and parallel model. The series model imposes a constant heat flux through each serially connected component (Figure 1a) so that each component develops different temperature gradients depending on its own thermal conductivity. In this case, the resistivity (inversion of conductivity) of the bulk material is the arithmetic average of the resistivity of each component weighted by their volume fractions (harmonic average for conductivity). The parallel model, on the other hand, imposes the identical temperature gradient to the individual phases or elements (Figure 1b) so that each phase has the same temperature difference, but conducts different heat flow depending on the thermal conductivity of each component. In this case, the thermal conductivity is the arithmetic mean of the thermal conductivity of each component. These two models are also referred to as upper and lower bounds (or Wiener bounds). They are the widest bounds with least constraint since no soil structure or fabric is considered. The larger the difference between the thermal conductivity values of each component, the wider the bandwidth of the bounds. Some other mixing laws also generate "averaged" effective thermal conductivity, such as the geometric mean law (hereafter Geo_Mean) and the quadratic parallel law (see Table 3).

Another group of mixing models can be derived based upon a combination of series and parallel models. *Mickley's (1951) model* (Mickley, 1951) involves a unit cubic cell (see Figure 2a) that consists of heat conduction through a $(1-a)^2$ solid block, heat conduction through a c^2 air block, and heat conduction through a series of solid, water film, and air, assuming a water film having a thickness of $b = a-c$. This model considers

unsaturated soil conditions by introducing the parameters a, b, c, which represent the proportions of solid, air, and water phases that can be determined for given porosity n and degree of saturation S. However, this method does not hold for very porous or dry soil, due to the poor grain-to-grain contacts when the soil is loose or few water bridges.

Woodside and Messmer's (1961) model (Woodside and Messmer, 1961) employed a three-component model that was originally used for determining electrical conductivity. The model visualizes three parallel heat flow paths in an idealized unit cube of soil as shown in Figure 2b. It consists of a path of width a through fluid and solid in series, a path of width b through continuous solid material, and a path of width c through continuous pore fluid. Given the thermal conductivity and volume fractions of each component, the key parameters a, b, c can be determined by porosity, and formation factor borrowed from Archie's law. This model only works for two-phase systems such as saturated soils, and determination of those parameters are difficult and by empirical fitting.

McGaw's (1969) model (McGaw, 1969) neglected the heat conduction through particle contacts and considered the heat flow mainly across solids with intervening fluid and passing entirely within the fluid (see Figure 2.c). This cubic cell can be expanded by adding one block in parallel for heat conducted in air. McGaw defined an interfacial efficiency factor ε (at solid/fluid interfaces), that turns to be close to 1- by assuming there is little temperature gradient within the intervening fluid, and the volume of this interfacial fluid n_c is about 0.03 for high saturation sand. To use this model, some

uncertain assumptions have to be made regarding the values of ε and n_c, when the soil is under low degrees of saturation.

Gori and Corasaniti's (2002) model (Gori and Corasaniti, 2002) used the cubic mixing model for thermal conductivity with considerations of different regimes of water content for three-phase soil in unsaturated conditions (see Figure 2d). The entire range of water content for a given soil is divided by the water content at the field capacity of the soil θ_f (when water has drained out of the larger pores but the small pores remain filled with water), water content at the permanent wilting point θ_p (water content at ~1.5 kPa of suction pressure), and water content of adsorbed water films θ_c (water film around the solid particles without connecting others, a fraction of θ_p). The model involves arrangement of the solid phase in the center of the gas cubic, with water films/bridges growing around the particle depending on the water content regime. The effective thermal conductivities of soils in each regime are defined separately by the mixing of air/water/solid phase. However, the dividing points were determined empirically for different types of soil.

Empirical Models

A number of empirical relationships between effective thermal conductivity and degree of saturation, porosity and soil types have been established by researchers. Kersten (Kersten, 1949) performed an extensive series of tests on various types of clays, silts and sands, and proposed empirical equations of thermal conductivity based on water content and dry bulk density for silt-clay and sandy soil with separate equations (see

Table 3). This empirical model leads to a discrepancy of ~25 % or higher for high silt-clay content soils and is only valid for the range of water content over which the experimental data is available.

Johansen introduced a normalized thermal conductivity called Kersten number K_e, given by $K_e = (k - k_{dry})/(k_{sat} - k_{dry})$ (Johansen, 1975). A model was developed by the relationships between the Kersten number and degree of saturation S. Simple first-order logarithmic functions of S for K_e were used to describe such relationships, where parameters in these equations were obtained by fitting the experimental results of different types of soils. To project the Kersten number to the effective thermal conductivity, the bounds at dry and saturated condition were calculated by thermal conductivity of single phase (solid, water, air) and other soil properties, such as dry bulk density, porosity, and quartz content. Johansen's model provided a method to estimate the effective thermal conductivity by interpolating between the dry and the saturated values of the thermal conductivity. Yet, issues come up when it applies to low quartz-content soils.

Inspired by the Johansen model, some other empirical models were derived based on the relative thermal conductivity described using the Kersten number K_e. Cote and Konrad modified the logarithmic equation into a hyperbolic equation for $K_e \sim S$ with a fitted material parameter κ, and redefined a new equation of determining dry thermal conductivity with two empirical parameters χ and η (Côté and Konrad, 2005). The *Cote and Konrad 2002 model* is applicable to more soil types and generates more accurate

estimation of thermal conductivity for the effective thermal conductivity than the *Johansen 1975 model*.

Other derivative models modified based upon the *Johansen's (1975) model* are *Lu et al.'s (2007) model* which used a modified exponential equation of saturation S with a fitted soil-type parameter α, and *Chen 2008 model* which adapted a modified power equation with two empirical parameters b and c to describe the effective thermal conductivity behavior with saturation S (Chen, 2008; Lu et al., 2007). These models better consider the tail behavior of thermal conductivity for fine-textured soil at low water content; however, lose applicability to other soil types.

Mathematical Models

This group of models usually is analog of other physical properties of mixtures, such as electrical conductivity, magnetic permittivity, elastic modulus (see Table 3). The *Hashin-Shtrikman's model*, hereinafter HS (Hashin and Shtrikman, 1962; Hashin and Shtrikman, 1963), employed variational principles and established the effective conductivity bounds that were first used for magnetic permeability and were found to be the best or narrowest possible bounds for composite materials, whose bulk properties could be derived from the property of the constituents and their volume fractions (Carson et al., 2005). The assumptions of HS model are that the composite materials are macroscopically homogeneous, isotropic, multi-phase, and it considers that the spheroidal intrusions are dispersed in a different matrix. It is referred to as "external porosity" material that the low conductivity spherical phase (e.g., air) dispersed in the high conductivity phase matrix (e.g., grains), restrained by the upper bound such as foams or sponges. The opposite case of high conductivity spherical phase (e.g., grains) dispersed in low conductivity matrix (e.g., air or water) is the "internal porosity" material such as soils, restrained by the lower bound (see schematic illustration in Figure 3.a). The HS upper and lower (HS_U, HS_L) bounds always lie within the parallel/series bounds discussed above, regardless of the component volume fractions or thermal conductivities.

The *Effective Medium Theory* (EMT), as one kind of the self-consistent method (SCM), has been proposed to distinguish the thermal conductivity region bounded by HS bounds into internal porosity and external porosity (Carson et al., 2005). The EMT model assumes that the bulk property of a composite material as a result of the interaction of

each phase is accounted for by imaging each phase to be an inclusion embedded in a homogeneous medium that has the overall property of the composite. It is equivalent to the composite has no continuous or dispersed phases with different conductivity; instead, the different phases are randomly distributed with the medium (see schematic illustration in Figure 3.b).

In summary, the *mixing models* are trying to simplify the soil microstructure and the arrangement of each phase into a simple combination of series and parallel elements in a representative elementary volume to substitute the apparent effective property of the bulk material. Although some more sophisticated models derived base on those mixing principle are trying to describe the effect of pore-water distribution (e.g., *Gori and Corasaniti's (2002) model*) or simulate the soil microstructure by fractal model (e.g., *Lehmann 2003 model,*(Lehmann et al., 2003)), they are basically lump the property of small elements into the effective bulk property without a realistic physical mechanism. The *empirical models* interpolate the effective thermal conductivity between the minimum value (dry thermal conductivity) and the maximum value (saturated thermal conductivity) by using different types of functions with empirical fitted parameter to apply different types of soil, whereas each model is only valid for a small group of soil type, and those parameters lack clear physical meanings, plus the determination of dry and saturated thermal conductivity were also not definite. The *mathematical models* approximate the effective thermal conductivity only by given property of each component and their volume fractions, by homogenization assumptions and analog of phase intrusion of a matrix in an electrical field or elastic energy conservation of

composite material under a field constrain, however, all of them have no consideration of the soil microstructure, solid particle geometry, water-phase distribution, and pore-size gradation.

Model Assessment by Experimental Data

In this section, the thermal conductivities of collected experimental data of different types of soil are compared with the prediction of the abovementioned models. Cross validation was used to evaluate each model. The properties of three types of soil used in the model predictions and assessments are listed in Table 5. The normalized root-mean-square-error (*NRMSE*) and the coefficient of variation of the root mean square error *CV*(*RMSE*) defined for the three sets of experimental data and the selected model predictions are summarized in Table 6. These values are defined as follows:

$$RMSE = \sqrt{\frac{\sum \left(k_{\exp} - k_{\mathrm{mod}} \right)}{n}} \tag{4}$$

$$NRMSE = \frac{RMSE}{k_{\exp}^{\max} - k_{\exp}^{\min}} \tag{5}$$

$$CV\left(RMSE\right) = \frac{RMSE}{\bar{k}_{\exp}} \tag{6}$$

The smaller the NRMSE number, the less the model prediction deviates from the measured data points.

A comparison of a set of measured thermal conductivity values for quartz sand and the calculated thermal conductivity by different models is shown in Figure 4 for the

conditions listed in Table 5. In Figure 4a, it can be clearly seen that the parallel/series models set the upper and lower limits of the possible thermal conductivity predictions. These two limits have the largest bandwidth, due to the large difference in the thermal conductivity values between the solid mineral and the air. The Geometric Mean model has an upward concave trend as the saturation increases, across the convex experimental data points. The HS upper and lower bounds lie within the parallel and series bounds, but still have large width and fail to capture the thermal conductivity variation pattern. All of the experimental data points fall into the external porosity region (lower than the SCM model, short dash-dot line). The SCM model is close to the experiment results only at high degrees of saturation. The De Vries' (1963) model underestimates the thermal conductivity at most of the range of saturation (De Vries, 1963). All the empirical models have similar calculation results of the thermal conductivity at different saturations. The relative thermal conductivity relations defined by the models of Johansen (1975), Cote's (2005) and Lu et al. (2007) use logarithmic, exponential and power functions, respectively, and have a similar trend with the measured data points. The functions describing those relations generate smooth curves and therefore cannot reflect the characteristic inflection points, which represent the critical saturation values dividing the pore-water distribution regimes, on the thermal conductivity curve for sand material. Figure 4b shows the 1:1 line for comparison of the measured and calculated results. None of the models have data points falling around the diagonal line throughout the entire range of saturation. The NRMSEs of all models are large (0.253 ~ 0.819), indicating that very large discrepancies exist between the experimental data and model predictions.

Although, the empirical models have lower NRMSE values than the other models, they still largely underestimate the thermal conductivity.

Figure 5 delineates the comparison of experimental measurements of sandy silt and model calculations. Evidently, the parallel/series and HS upper/lower bounds set the upper and lower limits of the thermal conductivity values. Geometric Mean model has the right trend but concaves to an opposite direction to the experimental data. SCM model has "quasi-linear" projections and higher predictions over all the saturation range. De Vries' (1963) model has close results at mediate saturation range 0.2 ~ 0.6. Empirical models are quite fit with the experimental data points. Nevertheless, only Lu et al.'s (2007) model captures the characteristic "flat-tail" behavior of thermal conductivity of silt at low degrees of saturation with a slightly shift. Also Johansen's and Lu et al.'s models underestimate the thermal conductivity at lower saturation and overestimate at higher saturation. Cote's model has the best fit with experimental data but fails to simulate the stasis behavior of thermal conductivity of silt at low degrees of saturation. Figure 5b shows the 1:1 diagonal comparison, and Cote's (2005) model has the lowest NRMSE value of 0.145.

Figure 6 shows the comparison of experimental data of clay soil and the model calculations. Parallel/Series model and the HS model again set the upper and lower bounds of the thermal conductivity for the multi-phase mixture. Geometric mean always cross the experimental curve and has the different shape of the curve. SCM model put all experimental data points into the "external porosity" zone between the SCM and HS_L line. Other mathematical models have higher calculation result than the experimental

results. All empirical models have monotonically increases of thermal conductivity simulation as the saturation increases, which are all far away from the true sigmoidal behavior for clay. Figure 6b shows the 1:1 diagonal comparison, with the NRMSE values ranging from 0.175 ~ 0.839.

By the above comparisons, the parallel/series bounds are much higher/lower than the real thermal conductivity of the sand measured throughout the saturation range. However, they set theoretical limits for all model predictions. The reason for that lies in the fact that the parallel/series models assume each of the components are stacked in layers to form the multiphase mixture. Those two represent the extreme cases of the heterogeneity of material and geometry. HS bounds have an additional constraint by assuming the second or other phases are uniformly dispersed in a continuous matrix. This homogenization technique generates more realistic upper and lower limits and thus narrows the bandwidth between two limits for the thermal conductivity of multiphase composites. However, water distribution in multiphase soil is generally non-uniform. SCM further lowers the upper bound by dividing the region bounded by HS model into “internal” and “external” porosity parts, making SCM model better in upper bound predictions. The thermal conductivities of soil at partially saturated conditions are always lower than SCM line where the “external porosity” region is resulted from the with high-thermal-conductivity soil particles “dispersed” in relatively low-thermal-conductivity air or water. This is not physically realistic in unsaturated soil. The Geometric Mean model averages the thermal conductivity of each phase in the unsaturated soil mixture but overestimates the contribution of pore-water at low degree of saturation and underestimate it at high degree

of saturation. The actual thermal conductivity for unsaturated soils evolves from the HS lower bound at dry and approaches to the SCM line at full saturation. As mentioned, the averaging and homogenization techniques do not consider the air-water interface and pore-water distribution in the soil at different stages of saturation. They do incorporate the governing factors of constituent, and water content (given the thermal conductivity of each phase and their volume fraction), but miss the factors of soil type and particle contacts (i.e., the influences of particle geometry, mineral type, and particle connectivity), and different water retention mechanisms for different saturations.

The empirical models use certain mathematical functions to fit the experimental results and then determine the parameters in these functions to match with certain type of soil. The difficulty of this group to apply all soil types is the uncertainty in calculating thermal conductivity of the solid minerals, which makes it harder to determine two end members, the thermal conductivity of dry and saturated states. Additionally, the smooth curves generated by logarithmic, exponential or power equations also cannot represent the different water retention regimes observed in different types of soil. The empirical models work better for silt and clay than sand, but are still far from accurate when soil has rich clay-content at low degrees of saturation. The empirical models integrate the key factors of constituent in terms of the thermal conductivities at dry state k_{dry} and at full saturated state k_{sat}, and consider the factor of water content, but still omit the factors of soil type and particle contact, which depends on the micro-structure of the material.

A Unified Conceptual Model

The change in thermal conductivity of soils with increasing degree of saturation differs remarkably for different soil types. For sandy soils, the thermal conductivity increases immediately once the soil experiences a small increase in degree of saturation, with a sharp jump to almost 70 % of the heat transfer capability at full saturation during wetting from dry conditions to approximately 5 % ~ 10 % degree of saturation. The increase in thermal conductivity becomes inconspicuous as the soil approaches fully saturated conditions. Inflection points are clearly observed for those separate regions at different critical degrees of saturation, indicating transition from one heat transfer mechanism to another.

For silt and clay soils, it can be observed that the thermal conductivity evolution with changing degree of saturation is much smoother than sand, without sharp inflection points. It can also be observed that the thermal conductivity values of silt or clay do not increase until the degree of saturation increases up to a certain threshold. The higher fines content of a soil, the longer the flat-tail development of thermal conductivity occurs at low degrees of saturation (e.g., clay has longer stasis development of thermal conductivity at low degrees of saturation, and therefore larger value of such threshold of saturation than silt). As the saturation continues increasing, the thermal conductivity gradually increases to gain most of the heat transfer capability in a short range of saturation (e.g. 5 % ~ 20 % for silt, and 35% ~ 55 % for clay in this case). Next, the thermal conductivity slowly increases to the maximum value and then keeps constant, as the saturation increases. Generally the thermal conductivity of silt and clay is lower than

that of the sand over the entire range of saturation, due to the lower thermal property of mineral constituents consist of fine soil than sands.

Based on the afore-mentioned analysis and observation, a conceptual model unifying thermal conductivity behavior and soil water retention mechanisms is proposed and shown in Figure 7. The full range of thermal conductivity variation with saturation can be distinguished and conceptualized in four regimes: hydration, pendular, funicular, and capillary. The range and boundary of each regime depends on the soil and liquid type and micro-structures (i.e., particle geometry, particle/pore size distribution, pore-water arrangement, and interfacial properties), which can be identified as the key governing factors shown in Table 2. These factors have been largely ignored in all the existing models. More importantly, these factors can also be characterized by the soil-water retention curve (SWRC). At thermodynamic or multiphase equilibrium for a given saturation, matric suction value indicates the information of certain pore size that holds certain amount of pore water of that soil. The characteristic changing of slopes and turning features on the SWRC curves reflect the effects of soil and liquid type and pore size distribution. Therefore, SWRC is a promising tool to unify all significant governing factors of the thermal conductivity of unsaturated soils for the proposed conceptual model.

As illustrated in Figure 7, from dry state to the first critical degree of saturation defines the hydration state (i.e., regime *1*), where only hydration water formed with the interaction of clay minerals. In this stage, water molecules are absorbed into mineral complex, which do not change the soil particle network or connectivity, thus the thermal properties of each constituent in soil. This is the physical reason why in rich fine-content

soil like silt and clay at the low degree of saturation, the thermal conductivity of bulk soil barely changes (e.g., S from 0 to 0.05 for silt or 0.35 for clay). The higher the fines content, the wider the range of this regime, and the higher value of this first critical saturation value. In the hydration regime, although pore water has been involved, the soil system behaves still like a two-phase mixture (solid/air), where the thermal conductivity follows the path close to the lower bounds (series/HS lower).

As the saturation increases, pore water starts to form thin film around the soil particle and build individual water bridges at the particle contacts, which is defined as pendular regime *2*. The water film/bridge overcomes the huge contact resistance in the dry soil-air-solid contact conduction and significantly improves the connectivity of thermal transfer paths, which contributes the rapid increase of the thermal conductivity. Sandy soil has very limited hydration stage; therefore the pendular regime dominates the low saturation region (e.g., $S = 0.05 \sim 0.1$). However, silty and clayey soil can have considerable amount of hydration water, which prevails the low saturation region and gradually transits to the pendular regime. The hydration water makes the thermal conductivity almost constant at the early stage of wetting, and the overlap between hydration and pendular regime makes the rapid smooth increase of thermal conductivity of silt or clay as the water content increase but not as steep as that of sand. The significant increase in water meniscus at the particle contacts is the physical reason why thermal conductivity in all types of soil increases rapidly within the pendular regime. The pendular regime can be $S = 0.05 \sim 0.15$ for silt or $0.35 \sim 0.55$ for clay. Of all the previous models, Only Cote's equation predicts closely to the measured data in this regime for silt. All empirical models fail to capture

the rapid change of the thermal conductivity of sand in this regime, and these models also cannot accurately predict thermal conductivity variations in clayey soil.

As the saturation continues to increase, the liquid bridges grow and begin to merge with adjacent ones and start to form a thick connected water-film around the soil particles, fill up the void space of pores. This regime carries on the buildup of the pore-water network, and this is the physical reason why the connectivity of heat transfer paths is further enhanced, leading to a gradual increase of thermal conductivity in funicular regime *3* (Figure 7). Because of the high thermal conductivity of solid minerals and the pore-water network, the heat flow goes in preference of the solid skeleton connected by pore-water at particle contacts. Hence, further increase of water content does not remarkably improve the thermal conductivity of the system as much as that in pendular regime. Here, the thermal conductivity of soil gradually increases to approach the maximum value (e.g., $S = 0.1 \sim 0.8$ for soil, $0.15 \sim 0.85$ for silt and $0.55 \sim 0.85$ for clay). The three empirical models have good fit in this section with silt, but underestimate the values of sand and overestimate the values of clay.

At even higher saturation, the pore-water occupies most of the voids instead of air, which does not further increase the thermal conductivity of the soil mixture in capillary regime *4* (Figure 7). In this regime, the increase of the pore water either does not further alter the preference of heat flow through the soil skeleton or improve the connectivity of heat transfer pathway. The range of capillary regime for sand is around $0.8 \sim 1$, and $0.85 \sim 1$ for silt and clay. From mediate to high degree of saturation, all models are converging to the upper bound (SCM line). Nevertheless for the empirical models, which

are better than others, the performance is limited by the accurate calculation the saturated thermal conductivity, which is estimated by a geometric mean of solid and liquid phase.

As shown, by linking the water retention mechanisms and thermal conductivity variation behavior, and by comparing the previous models with the experimental data for different types of soil, the large discrepancies predicted by the previous models lay in the overlook of the roles of different water retention regimes in thermal conductivity variation. None of the models explicitly used the governing factors of soil and liquid types and pore size distribution that characterize the soil water retention. The existing models are all pore-structure independent. In two-phase systems, the previous theoretical models are close to experiment results for certain type of soil. However, when air and water are both involved, the complexity of pore-water network and connections is increased due to the air-water interfaces. How water phase distributed in the pore space at different degrees of saturation defines the connectivity of the pore water in the soil skeleton and therefore determines the thermal behavior of unsaturated soils.

Conclusions

This paper reviews the existing models of thermal conductivity for unsaturated soil, assess these models' predictability, and thereby identify the controlling factors for thermal conduction in porous media. The existing thermal conductivity models are assessed and categorized into three groups based on their assumptions and principles. *Mixing models* simulate the thermal conductivity of mixtures by a combination of simple parallel or series elements consisting of the composite. *Mathematical models* adopt the

homogenization approaches to calculate the thermal conductivity of a uniform composite. *Empirical models* use different functions to fit the experimental measurements and their parameters to apply to certain soil types. All model predictions are compared with experimental data of three types of unsaturated soil: sand, silt and clay. It is found that these models are either work only at portions of saturation range or apply to certain soil type. Most importantly, these models lack the consideration of some key governing factors such as soil and liquid type and pore size distribution. It is found that the pore-scale water distribution based on thermodynamic equilibrium conditions among air-water-solid interfaces during different saturation states have not been reflected in all the existing models.

A conceptual model is proposed based on the analysis of heat transfer mechanisms and the discussion about missing factors from existing models in terms of the effect of pore water distribution at different water retention regimes. These water retention regimes are governed by the SWRC and can be used to fully reconcile variations of thermal conductivity with degree of saturation for all types of soil. Quantitative linkages between the pore size distribution, soil-water interaction mechanisms, and the bulk thermal conductivity variation behavior can be established in light of the SWRC.

Acknowledgements

The funding for this research is provided by a grant from National Science Foundation (NSF-CMMI-1230544) to JSM and NL.

References

Aduda, B.O., 1996, Effective thermal conductivity of loose particulate systems. Journal of Materials Science, 31: 6441-6448.

Brandl, H., 2006, Energy foundations and other thermo-active ground structures. Geotechnique, 56: 81-122.

Brandon, T.L. and Mitchell, J.K., 1989, Factors Influencing Thermal Resistivity of Sands. Journal of Geotechnical Engineering, 115.

Carslaw, H. and Jaeger, J., 1959, Conduction of Heat in Solids (paperback,).

Carson, J.K., Lovatt, S.J., Tanner, D.J. and Cleland, A.C., 2005, Thermal conductivity bounds for isotropic, porous materials. International Journal of Heat and Mass Transfer, 48: 2150-2158.

Chen, S., 2008, Thermal conductivity of sands. Heat and Mass Transfer, 44: 1241-1246.

Cortes, D.D., Martin, A.I., Yun, T.S., Francisca, F.M., Santamarina, J.C. and Ruppel, C., 2009, Thermal conductivity of hydrate-bearing sediments. Journal of Geophysical Research, 114: B11103.

Côté, J. and Konrad, J.-M., 2005, A generalized thermal conductivity model for soils and construction materials. Canadian Geotechnical Journal, 42: 443-458.

De Vries, D.A., 1963, Thermal properties of soils. In: VAN WIJK, W.R. (ed.), Physics of Plant Environment. Wiley, New York, 210–235.

Ebigbo, A., 2005, Thermal effects of carbon dioxide sequestration in the subsurface, Master's thesis, Institut für Wasserbau, Universität Stuttgart

Esch, D.C., 2004, Thermal analysis, construction, and monitoring methods for frozen ground. ASCE Publications

Farouki, O.T., 1981, Thermal Properties of Soils, Report

Gangadhara Rao, M. and Singh, D.N., 1999, A generalized relationship to estimate thermal resistivity of soils. Canadian Geotechnical Journal, 36: 767-773.

Gori, F. and Corasaniti, S., 2002, Theoretical Prediction of the Soil Thermal Conductivity at Moderately High Temperatures. Journal of Heat Transfer-transactions of The Asme, 124.

Hashin, Z. and Shtrikman, S., 1962, A Variational Approach to the Theory of the Effective Magnetic Permeability of Multiphase Materials. Journal of Applied Physics, 33: 3125-3131.

Hashin, Z. and Shtrikman, S., 1963, A variational approach to the theory of the elastic behaviour of multiphase materials. Journal of the Mechanics and Physics of Solids, 11: 127-140.

Johansen, O., 1975, Thermal conductivity of soils, University of Trondheim, Trondheim, Norway.

Kersten, M.S., 1949, Laboratory research for the determination of the thermal properties of soils, Report, DTIC Document.

Lambert, M.A. and Fletcher, L.S., 1997a, Thermal Contact Conductance of Spherical Rough Metals. Journal of Heat Transfer-transactions of The Asme, 119.

Lambert, M.A. and Fletcher, L.S., 1997b, Review of Models for Thermal Contact Conductance of Metals. Journal of Thermophysics and Heat Transfer, 11: 129-140.

Lehmann, P., Stähli, M., Papritz, A., Gygi, A. and Flühler, H., 2003, A Fractal Approach to Model Soil Structure and to Calculate Thermal Conductivity of Soils. Transport in Porous Media, 52: 313-332.

Li, D., Sun, X. and Khaleel, M., 2012, Comparison of Different Upscaling Methods for Predicting Thermal Conductivity of Complex Heterogeneous Materials System: Application on Nuclear Waste Forms. Metallurgical and Materials Transactions A: 1-9.

Lu, S., Ren, T., Gong, Y. and Horton, R., 2007, An Improved Model for Predicting Soil Thermal Conductivity from Water Content at Room Temperature. Soil Science Society of America Journal, 71.

McGaw, R., 1969, Heat conduction in saturated granular materials. Highway Research Board Special Report.

Mickley, A., 1951, The thermal conductivity of moist soil. American Institute of Electrical Engineers, Transactions of the, 70: 1789-1797.

Mitchell, J.K. and Soga, K., 2005, Fundamentals of soil behavior. John Wiley & Sons Inc, New York.

Murashov, V.V. and White, M., 2000, Thermal conductivity of crystalline particulate materials. Journal of Materials Science, 35: 649-653.

Preene, M. and Powrie, W., 2009, Ground energy systems: from analysis to geotechnical design. Geotechnique, 59: 261-271.

Sahimi, M. and Tsotsis, T.T., 1997, Transient Diffusion and Conduction in Heterogeneous Media: Beyond the Classical Effective-Medium Approximation. Industrial & Engineering Chemistry Research, 36: 3043-3052.

Singh, D.N. and Devid, K., 2000, Generalized relationships for estimating soil thermal resistivity. Experimental Thermal and Fluid Science, 22: 133-143.

Smits, K.M., Sakaki, T., Limsuwat, A. and Illangasekare, T.H., 2010, Thermal Conductivity of Sands under Varying Moisture and Porosity in Drainage–Wetting Cycles. Vadose Zone Journal, 9: 172-180.

Tarnawski, V.R., Leong, W.H., Gori, F., Buchan, G.D. and Sundberg, J., 2002, Interparticle contact heat transfer in soil systems at moderate temperatures. International Journal of Energy Research, 26: 1345-1358.

Tarnawski, V.R., Momose, T. and Leong, W.H., 2009, Assessing the impact of quartz content on the prediction of soil thermal conductivity. Geotechnique, 59: 331-338.

Vargas, W.L. and McCarthy, J.J., 2001, Heat conduction in granular materials. AIChE Journal, 47: 1052-1059.

White, D.E., 1973, Characteristics of geothermal resources. Geothermal Energy, Stanford University Press, Stanford: 69-94.

Woodside, W. and Messmer, J.H., 1961, Thermal Conductivity of Porous Media. I. Unconsolidated Sands. Journal of Applied Physics, 32: 1688-1699.

Yun, T.S., 2005, Mechanical and Thermal Study of Hydrate Bearing Sediments, Ph.D., Georgia Institute of Technology, Atlanta

Yun, T.S. and Santamarina, J.C., 2008, Fundamental study of thermal conduction in dry soils. Granular Matter, 10: 197.

List of Tables and Figures

uses solid lines, group II dot-dash lines, and group III dot lines), and (b) 1:1 comparison space for predicted and measured values (group I uses symbols -, +, x; group II hollow symbols □, ◊, Δ, ○; group III solid-filled symbols □, Δ, ○).

Figure 6. Comparison of thermal conductivity model simulation and the experimental data of clay: (a) effective thermal conductivity with degree of saturation (group I uses solid lines, group II dot-dash lines, and group III dot lines), and (b) 1:1 comparison space for predicted and measured values (group I uses symbols -, +, x; group II hollow symbols □, ◊, Δ, ○; group III solid-filled symbols □, Δ, ○).

Figure 7. Conceptual model of thermal conductivity: (a) thermal conductivity and soil-water retention, and (b) regimes of pore-water distribution.

Figure
Click here to download Figure: Dong et al Tables and Figures.doc

Table 1

Material	Density [kg/m^3]	Heat capacity [kJ/kg·K]	Thermal conductivity [W/m·K]	Thermal diffusivity [m^2/s] x 10^{-7}
Air (10 ^{o}C)	1.25	1.000	0.0026	0.21
Water (25 ^{o}C)	999.87	4.200	0.56	1.43
Water vapor (1 atm, 400 K)	-	1.901	0.016	233.8
Ice (0 ^{o}C)	917	2.040	2.25	12
Quartz	2660	0.733	8.40	43.08
Granite	2750	0.890	1.70 ~ 4.00	~ 12
Gypsum	1000	1.090	0.51	4.7
Limestone	2300	0.900	1.26 ~ 1.33	~5
Marble	2600	0.810	2.80	13
Mica	2883	0.880	0.75	2.956
Clay	1450	0.880	1.28	10
Sandstone	~ 2270	0.710	1.60 ~ 2.10	10 ~ 13

Source: Bejan, Adrian; Kraus, Allan D. (2003). Heat Transfer Handbook. John Wiley & Sons.

Table 2

Key governing factors	Features
Constituent	• Thermal conductivity of solid minerals dominates the bulk property.
Soil type	• ifferent type of soil has different soil minerals, particle sizes and shapes.
Water content	• The volume fraction of water phase determines the thermal conductivity of partially saturated soils.
Particle contact	• The coordination number affected by stress level, packing density, gradation et al. defines the thermal conduction skeleton.

Table 3

Models	Equations
Series	$\frac{1}{k_{\text{eff}}} = \sum_{i=1}^{3} \phi_i \cdot \frac{1}{k_i}$
Parallel	$k_{\text{eff}} = \sum_{i=1}^{3} \phi_i \cdot k_i$
Geometric mean	$k_{\text{eff}} = \prod_{i=1}^{3} k_i^{\phi_i}$
Quadratic parallel	$k_{\text{eff}} = \left(\sum_{i=1}^{3} \phi_i \cdot \sqrt{k_i} \right)^2$
Effective medium	$\sum_{i}^{3} \left(\phi_i \frac{k_i - k_{\text{eff}}}{k_i + 2k_{\text{eff}}} \right) = 0$
Self-consistent	$k_{\text{eff}} = \frac{1}{3} \left(\sum_{i=1}^{3} \frac{\phi_i}{k_i + 2k_{\text{eff}}} \right)^{-1}$
De Vries (1963)	$k_{\text{eff}} = \frac{\phi_{\text{w}} k_{\text{w}} + F_{\text{s}} \phi_{\text{s}} k_{\text{s}} + F_{\text{a}} \phi_{\text{a}} k_{\text{a}}}{\phi_{\text{w}} + F_{\text{s}} \phi_{\text{s}} + F_{\text{a}} \phi_{\text{a}}}$, F_i and g_i are weight and shape factors
Hashin-Strikmann	$k_{\text{HS}}^{L} = k_1 + 3k_1 \frac{\sum_{i=2}^{3} \left(\phi_i / \left(1 + c_i^{L} \right) \right)}{\phi_1 + \sum_{i=2}^{3} \left(\phi_i c_i^{L} / \left(1 + c_i^{L} \right) \right)}$, $c_i^{L} = 3k_1 / \left(k_i - k_1 \right)$, $k_{\text{HS}}^{U} = k_3 + 3k_3 \frac{\sum_{i=1}^{2} \left(\phi_i / \left(1 + c_i^{U} \right) \right)}{\phi_3 + \sum_{i=1}^{2} \left(\phi_i c_i^{U} / \left(1 + c_i^{U} \right) \right)}$, $c_i^{U} = 3k_3 / \left(k_i - k_3 \right)$

Key factors:
ϕ_i - volume fraction of each phase, i can be a (air) w (water) s (solid), [-]
k_i - thermal conductivity of each phase, (k_a = 0.56, k_w = 0.026), [W/mK]

Table 4

Models	Parameters						Equations
	k_i	S (θ)	n	γ_{dry}	k_e, k_{dry}, k_{sat}	others	
Kersten (1949)		–		–			Silt-clay: $k_{eff} = 0.1442(\log\theta - 0.2)\cdot 10^{0.6243\cdot\gamma_{dry}}$ Sandy soil: $k_{eff} = 0.1442(\log\theta - 0.2)\cdot 10^{0.6243\cdot\gamma_{dry}}$
Johansen (1975)	$k_s = k_q^q k_o^{(1-q)}$	–	–	–	$k_{sat} = k_s^{(1-n)} k_w^n$ $k_{dry} = \frac{0.135\gamma_{dry} + 64.7}{2700 + 0.947\gamma_{dry}}$		Coarse sand: $k_e = 0.7\log S + 1.0$ Fine soil: $k_e = \log S + 1.0$
Cote (2005)	$k_s = k_q^q k_o^{(1-q)}$	–	–	–	$k_{sat} = k_s^{(1-n)} k_w^n$ $k_{dry} = \chi\times 10^{-\eta\cdot n}$	χ	$k_e = \frac{\kappa S}{1 + (\kappa - 1)S}$
Lu (2007)	$k_s = k_q^q k_o^{(1-q)}$	–	–	–	–	α	$k_e = \exp\left[\alpha\left(1 - S^{\alpha - 1.33}\right)\right]$
Chen (2008)	–	–	–			b, c	$k_{eff} = k_s^{1-n} k_w^n n\cdot\left[(1-b)S + b\right]^{cn}$

Key parameters:
S - degree of saturation, $S = \square_w/(1 - \square_s)$, [-]
θ – volumetric water content, $\theta = (n\cdot S)$, [-]
n - porosity, n = $(1 - \square_s)$, [-]
γ_{dry} - dry bulk density, $\gamma_{dry} = G_s(1 - n)$, [kg/m^3]
k_q - thermal conductivity of quartz, [W/mK]
k_o - thermal conductivity of organic materials, [W/mK]
k_e – Kersten number, $k_e = (k_{eff} - k_{dry})/(k_{sat} - k_{dry})$, [-]

Empirical parameters:
α, χ, b, c – fitted parameters for different materials

Table 5

Experimental Data		Parameters					
		k_s[W/mK]	G_s[unitless]	n[unitless]	γ_{dry}[kg/m^3]	k_{dry}[W/mK]	k_{satl}[W/mK]
Sands	Accusand 40/50	4.75	2.65	0.37	1.696	0.07/0.28	2.27
Silt	Bonny silt	2.5	2.53	0.39	1.25	0.06/0.26	1.42
Clay	Tamawaski (2002)	2.5	2.65	0.5	1.325	0.06/0.19	1.18

Table 6

Cross validation		Mixing models			Mathematical models				Empirical models		
		Parallel	Series	Geo_Mean	HS_L	HS_U	SCM	De Vries 1952	Johansen 1975	Cote 2005	Lu 2007
Sand	NRMSE	0.631	0.819	0.395	0.747	0.456	0.333	0.253	0.374	0.282	0.330
	CV(RMSE)	0.745	0.966	0.466	0.881	0.538	0.393	0.299	0.441	0.333	0.389
Silt	NRMSE	1.019	0.788	0.219	0.628	0.769	0.576	0.295	0.224	0.145	0.310
	CV(RMSE)	1.097	0.848	0.236	0.676	0.828	0.620	0.317	0.241	0.156	0.334
Clay	NRMSE	0.839	0.612	0.175	0.462	0.635	0.437	0.311	0.297	0.355	0.255
	CV(RMSE)	0.997	0.728	0.208	0.549	0.755	0.520	0.370	0.353	0.422	0.303

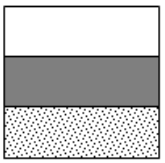

$$k_{\text{eff}} = \sum_{i=1}^{3} (\phi_i \cdot k_i)$$

Series (Wiener lower)

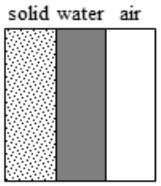

$$\frac{1}{k_{\text{eff}}} = \sum_{i=1}^{3} \left(\frac{\phi_i}{k_i} \right)$$

Parallel (Wiener upper)

Figure 1

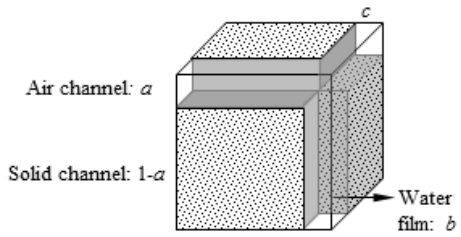

$$k_{\text{eff}} = k_a \cdot c^2 + k_s \cdot (1-a)^2 + k_w \cdot b^2 + \frac{2k_w k_a cb}{k_w c + k_a (1-c)} + \frac{2k_s k_w (1-a) b}{k_s a + k_a (1-a)} + \frac{2k_s k_w k_a (1-a) c}{k_s k_w c + k_s k_a b + k_w k_a (1-a)}$$

where: $\begin{cases} 3a^2 + 2a^3 = n \\ 3c^2 - 2c^3 = (1-S)n \\ c = a - b \end{cases}$

(a)

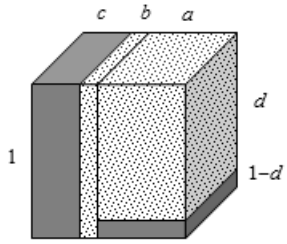

$$k_{\text{eff}} = k_s \cdot b + k_w \cdot c + \frac{k_w k_s a}{k_w d + k_s (1-d)}$$

where: $\begin{cases} a + b + c = 1 \\ b + ad = 1 - n \end{cases}$

(b)

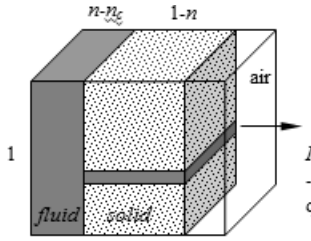

$$k_{\text{eff}} = k_w \cdot (nS - n_c) + (1 - n + n_c) \frac{\varepsilon k_s (1 - n + n_c)}{(1-n) + n_c \frac{k_s}{k_w}} + (n - nS) k_a$$

where: $\varepsilon = 1 - \frac{\Delta T_i}{\Delta T}$

(c)

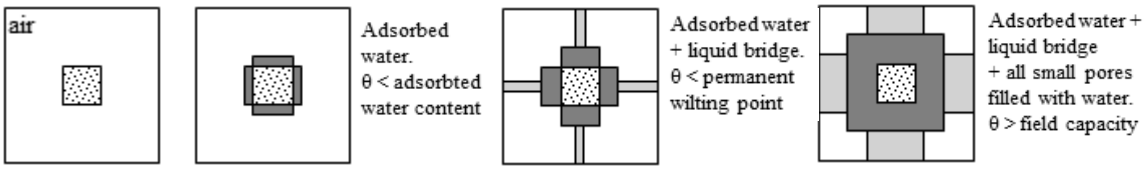

(d)

Figure 2

(a) 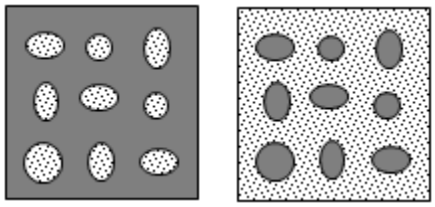

(b) 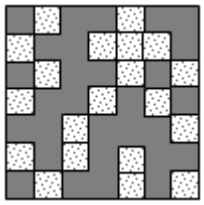

Figure 3

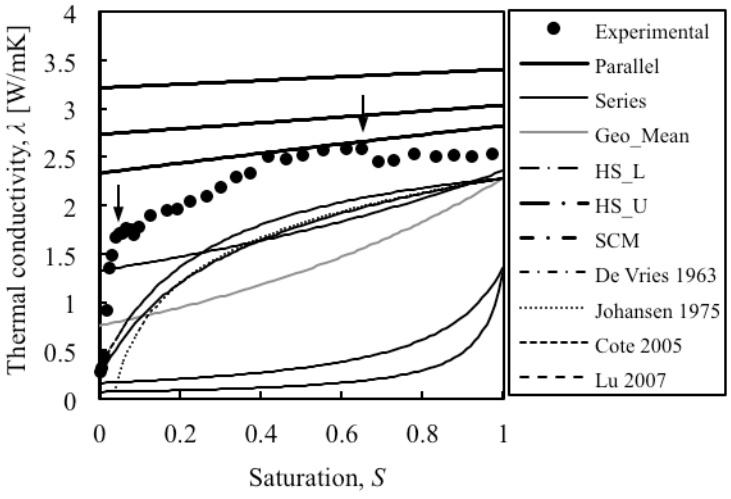
Thermal conductivity, λ [W/mK]
Saturation, S
Experimental
Parallel
Series
Geo_Mean
HS_L
HS_U
SCM
De Vries 1963
Johansen 1975
Cote 2005
Lu 2007

(a)

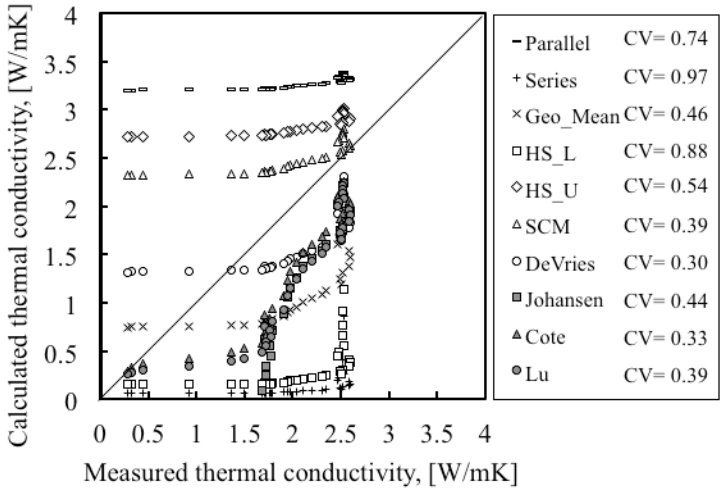
Calculated thermal conductivity, [W/mK]
Measured thermal conductivity, [W/mK]
Parallel CV= 0.74
Series CV= 0.97
Geo_Mean CV= 0.46
HS_L CV= 0.88
HS_U CV= 0.54
SCM CV= 0.39
DeVries CV= 0.30
Johansen CV= 0.44
Cote CV= 0.33
Lu CV= 0.39

(b)

Figure 4

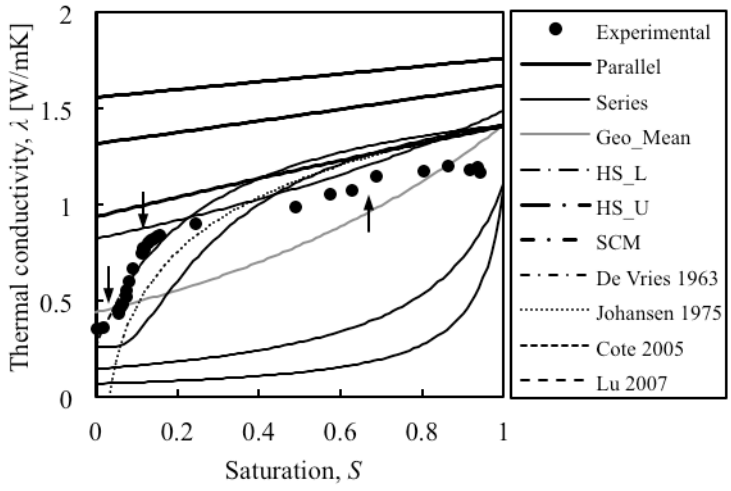
Thermal conductivity, λ [W/mK]
Saturation, S
Experimental
Parallel
Series
Geo_Mean
HS_L
HS_U
SCM
De Vries 1963
Johansen 1975
Cote 2005
Lu 2007

(a)

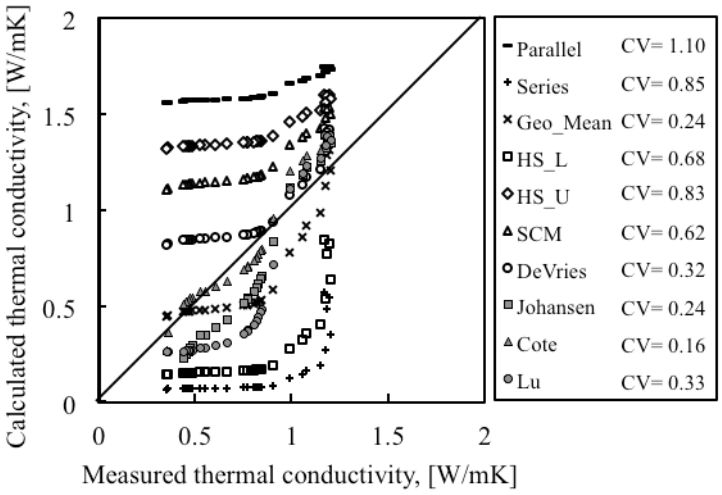
Calculated thermal conductivity, [W/mK]
Measured thermal conductivity, [W/mK]
Parallel CV= 1.10
Series CV= 0.85
Geo_Mean CV= 0.24
HS_L CV= 0.68
HS_U CV= 0.83
SCM CV= 0.62
DeVries CV= 0.32
Johansen CV= 0.24
Cote CV= 0.16
Lu CV= 0.33

(b)

Figure 5

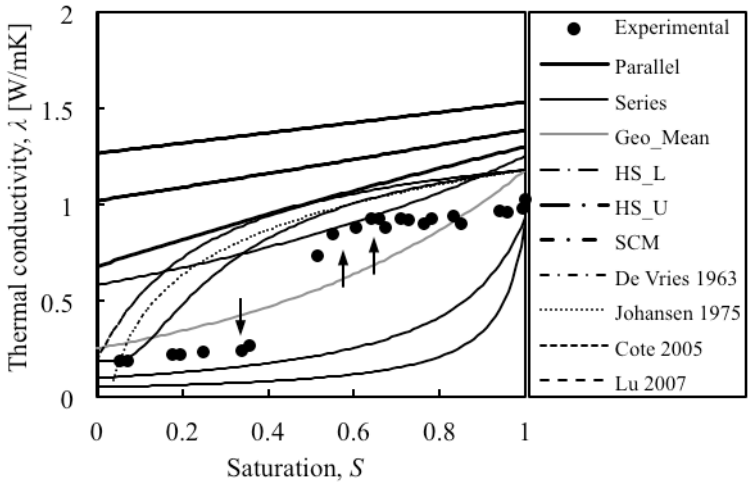
Thermal conductivity, λ [W/mK]
Saturation, S
Experimental
Parallel
Series
Geo_Mean
HS_L
HS_U
SCM
De Vries 1963
Johansen 1975
Cote 2005
Lu 2007

(a)

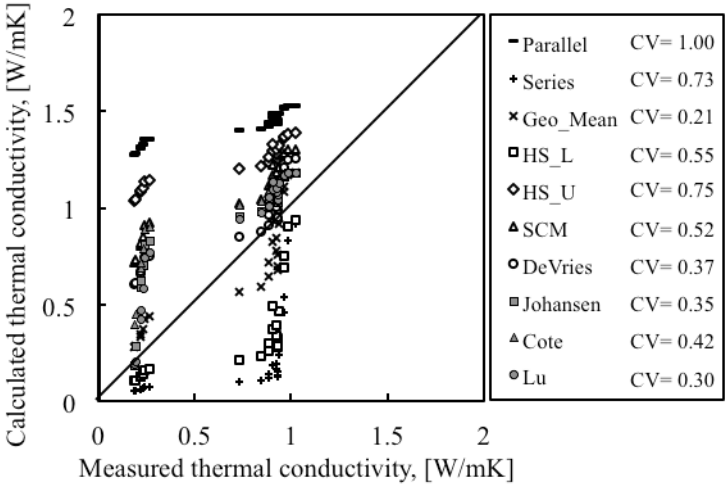
Calculated thermal conductivity, [W/mK]
Measured thermal conductivity, [W/mK]
Parallel CV= 1.00
Series CV= 0.73
Geo_Mean CV= 0.21
HS_L CV= 0.55
HS_U CV= 0.75
SCM CV= 0.52
DeVries CV= 0.37
Johansen CV= 0.35
Cote CV= 0.42
Lu CV= 0.30

(b)

Figure 6

(a)

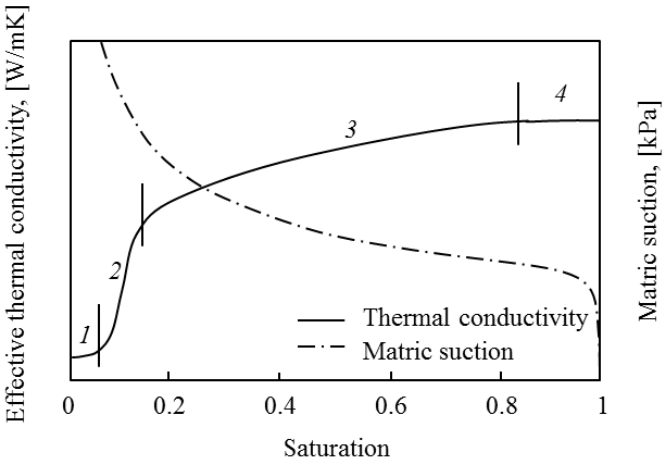
Effective thermal conductivity, [W/mK]
Matric suction, [kPa]
Saturation
0
0.2
0.4
0.6
0.8
1
1
2
3
4
Thermal conductivity
Matric suction

(b)

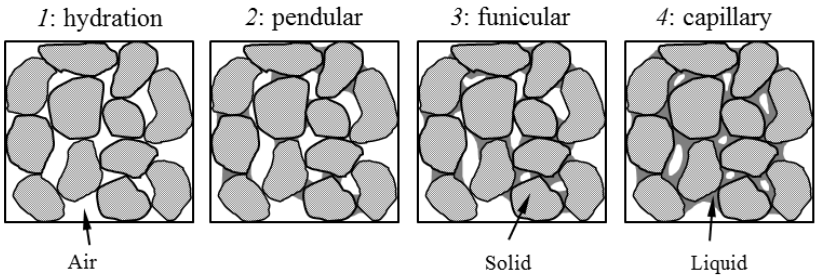
1: hydration
2: pendular
3: funicular
4: capillary
Air
Solid
Liquid

Figure 7